

General Disclaimer

One or more of the Following Statements may affect this Document

- This document has been reproduced from the best copy furnished by the organizational source. It is being released in the interest of making available as much information as possible.
- This document may contain data, which exceeds the sheet parameters. It was furnished in this condition by the organizational source and is the best copy available.
- This document may contain tone-on-tone or color graphs, charts and/or pictures, which have been reproduced in black and white.
- This document is paginated as submitted by the original source.
- Portions of this document are not fully legible due to the historical nature of some of the material. However, it is the best reproduction available from the original submission.

DRD No. RE-5
DEL No. 139

**LARGE-AREA SHEET TASK
ADVANCED DENDRITIC WEB GROWTH DEVELOPMENT**

9950-724

C. S. Duncan, R. G. Saldensticker, J. P. McHugh,
R. H. Hopkins, D. Maier, and J. Schruben

Quarterly Report

October 24, 1981 to December 31, 1981

June 18, 1982

Dist. Category UC63
DOE/JPL-955843/82/5

Contract No. 955843

The JPL Flat Plate Solar Array Project is sponsored by the U. S. Dept. of Energy and forms part of the Solar Photovoltaic Conversion Program to initiate a major effort toward the development of low-cost solar arrays. This work was performed for the Jet Propulsion Laboratory, California Institute of Technology, by agreement between NASA and DOE.

(NASA-CR-169624) LARGE-AREA SHEET TASK
ADVANCED DENDRITIC WEB GROWTH DEVELOPMENT
Quarterly Report, 24 Oct. - 31 Dec. 1981
(Westinghouse Research and) 23 p
HC A02/MF A01

N83-14665

Unclas
01675

CSCL 10A G3/44



Westinghouse R&D Center
1310 Beulah Road
Pittsburgh, Pennsylvania 15235

DRD No. SE-5
DRL No. 139

**LARGE-AREA SHEET TASK
ADVANCED DENDRITIC WEB GROWTH DEVELOPMENT**

**C. S. Duncan, R. G. Seidensticker, J. P. McHugh,
R. H. Hopkins, D. Meier, and J. Schruben**

Quarterly Report

October 24, 1981 to December 31, 1981

June 18, 1982

**Dist. Category UC63
DOE/JPL-955843/82/5**

Contract No. 955843

The JPL Flat Plate Solar Array Project is sponsored by the U. S. Dept. of Energy and forms part of the Solar Photovoltaic Conversion Program to initiate a major effort toward the development of low-cost solar arrays. This work was performed for the Jet Propulsion Laboratory, California Institute of Technology, by agreement between NASA and DOE.



**Westinghouse R&D Center
1310 Beulah Road
Pittsburgh, Pennsylvania 15235**

CONTENTS

List of Figures.....	iii
1. SUMMARY.....	1
2. INTRODUCTION.....	2
3. TECHNICAL PROGRESS.....	4
3.1 Modeling of Dendritic Web Growth.....	4
3.1.1 Synthetic Temperature Profile Results.....	4
3.1.2 Design of J419 Growth Configuration.....	8
3.2 New Experimental Web Growth Facility.....	12
4. CONCLUSIONS.....	14
5. PLANS AND FUTURE WORK.....	15
6. NEW TECHNOLOGY.....	15
7. REFERENCE.....	15
8. ACKNOWLEDGEMENTS.....	15
9. PROGRAM SCHEDULE AND COSTS.....	16

LIST OF FIGURES

	Page
Figure 1 Constant stress temperature profiles.....	6
Figure 2 End effect region of constant stress profile.....	7
Figure 3 Stresses generated by abruptly changing zero stress temperature profiles.....	9
Figure 4 J419 configuration.....	11

PRECEDING PAGE BLANK NOT FILMED

1. SUMMARY

During this quarter, the thermal stress model was used to generate the design of a low-stress lid and shield configuration, which was fabricated and tested experimentally. The results agreed with the predictions of the buckling model and crystals were grown to a width of 49.9 mm.

In preliminary tests, the New Experimental Web Growth Facility performed as designed, producing web on the first run. These experiments suggested desirable design modifications in the melt level sensing system to improve further its performance, and these are being implemented.

2. INTRODUCTION

Silicon dendritic web is a single crystal silicon ribbon material which provides substantial advantages for low-cost manufacture of solar cells. A significant feature of the process is the growth from a melt of silicon without constraining dies, resulting in an oriented single crystal ribbon having excellent surface features. In common with other more classical processes such as Czochralski growth, impurity rejection into the melt permits the use of less pure "solar grade" starting material without significantly affecting cell performance. A unique property of the dendritic web process is the growth of long ribbons of controllable width and thickness which not only facilitates automation of subsequent processing into solar cells, but also results in high material utilization since cutting and polishing are not required.

On the present contract, three broad areas of work are emphasized:

1. The development of thermal stress models in order to understand the detailed parameters which generate buckling stresses. The model can then be used to guide the design of improved low-stress web growth configurations for experimental testing.
2. Experiments to increase our understanding of the effects of various parameters on the web growth process.
3. The construction of an experimental web growth machine which contains in a single unit all the mechanical and electronic features developed previously so that experiments can be carried out under tightly controlled conditions.

Thus, the principal objective of this work has been to expand our knowledge and understanding of both the theoretical and experimental aspects of the web growth process to provide a solid base for substantial improvements in both area throughput and web crystal quality.

During this reporting period, the modeling results were used as the basis for the design of a new lid and shield configuration. Experimental evaluation of this design gave results in almost perfect agreement with the predictions of the model.

3. TECHNICAL PROGRESS

3.1 Modeling of Dendritic Web Growth

Previous studies of thermal stress and buckling have used mathematical models to evaluate the performance of real, or at least proposed, lid and shield configurations. This type of analysis was continued during the present period but, in addition, stresses were computed for several temperature distributions which were synthesized purely on the basis of their mathematical properties. These "synthetic" temperature profiles were evaluated to illustrate the requirements of a low-stress profile.

3.1.1 Synthetic Temperature Profile Results

Boley and Wiener(1) have published an often-cited series solution for the stress components in a uniform ribbon having a temperature distribution varying only with x (the coordinate along the length of the ribbon). The first term of their result for σ_{xx} is

$$\sigma_{xx} = \frac{\alpha E w^2}{6} \left(3 - \frac{y^2}{w^2} \right) T'' \quad [1]$$

where α is the thermal expansivity (assumed to be constant), E is Young's modulus (also constant), w is the half width of the ribbon, and y is the width coordinate. The prediction of equation 1, that $\sigma_{xx} = 0$ if $T'' = 0$, does not hold if the thermoelastic properties (α or E) vary with temperature; for our calculations we assume that E is constant but allow α to depend on temperature. The condition for zero stress is then $(\alpha T)'' = 0$, and for constant stress, equation 1 becomes

$$(\alpha T)'' = 6\sigma_{xx}/E(3w^2 - y^2) \quad [2]$$

By assuming an analytic form for $\alpha(T)$, e.g., $\alpha = \alpha_0 + \alpha_1 T$, equation 2 can be solved to identify temperature distributions giving constant stress in the ribbon. A series of such temperature distributions is shown in Figure 1, where the parameter labeling the curves is the difference in stress between the ribbon center and ribbon edge.

The series solution from which equation 1 was derived only applies when end effects are negligible and when T'' (or $(\alpha T)''$) is not changing rapidly. Both of these conditions are violated near the growth front of the dendritic web. Since essentially zero tension is applied to the growing interface, the growth front is a traction-free boundary. Further, because of the rapidly changing high temperature of the ribbon in this region, T'' also changes rapidly. In order to develop at least a semi-quantitative understanding of the effect of these two conditions on the thermal stresses, two "synthetic" temperature profiles were used as input data for the WECAN stress calculations.

To illustrate the effect of the traction-free boundary, a temperature profile was used that would generate a constant stress according to equation 2. The traction-free boundary condition was intrinsic to the WECAN analysis used for the calculation.

The result is shown in Figure 2, which depicts $\Delta\sigma_{xx}$ along the ribbon. This stress parameter was chosen since it reduces the "grain" inherent in the finite element calculations. From simple inspection of the curve, it can be seen that the end effect of the free boundary extends for a distance approximately equal to the ribbon width (2.7 cm in this calculation). Although the fit is not exact, the effect of the boundary seems to be approximately a complementary Gaussian with a characteristic length equal to the ribbon width. This result shows that the details of the $(\alpha T)''$ curve near the growth front are mitigated to a large extent by the end effect. This may be of importance in future

ORIGINAL PAGE IS
OF POOR QUALITY

Curve 730152-A

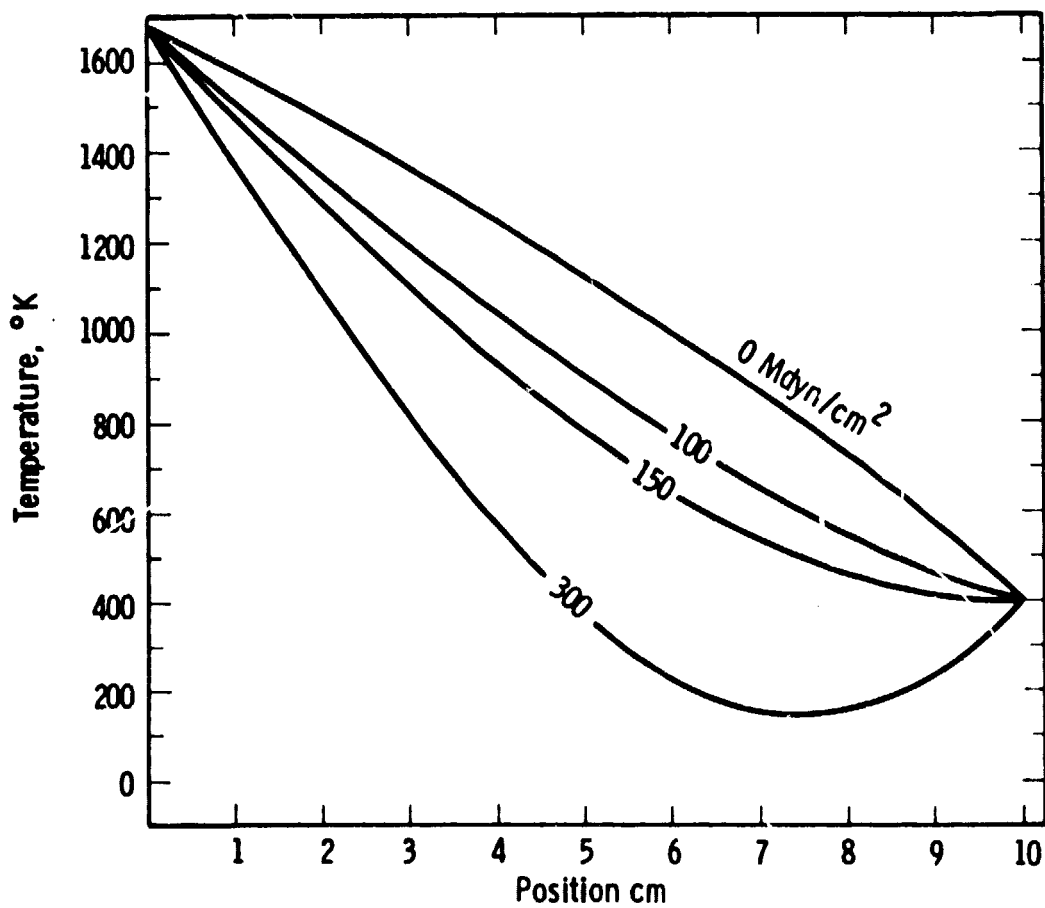


Figure 1. Constant stress temperature profiles.

ORIGINAL PAGE IS
OF POOR QUALITY

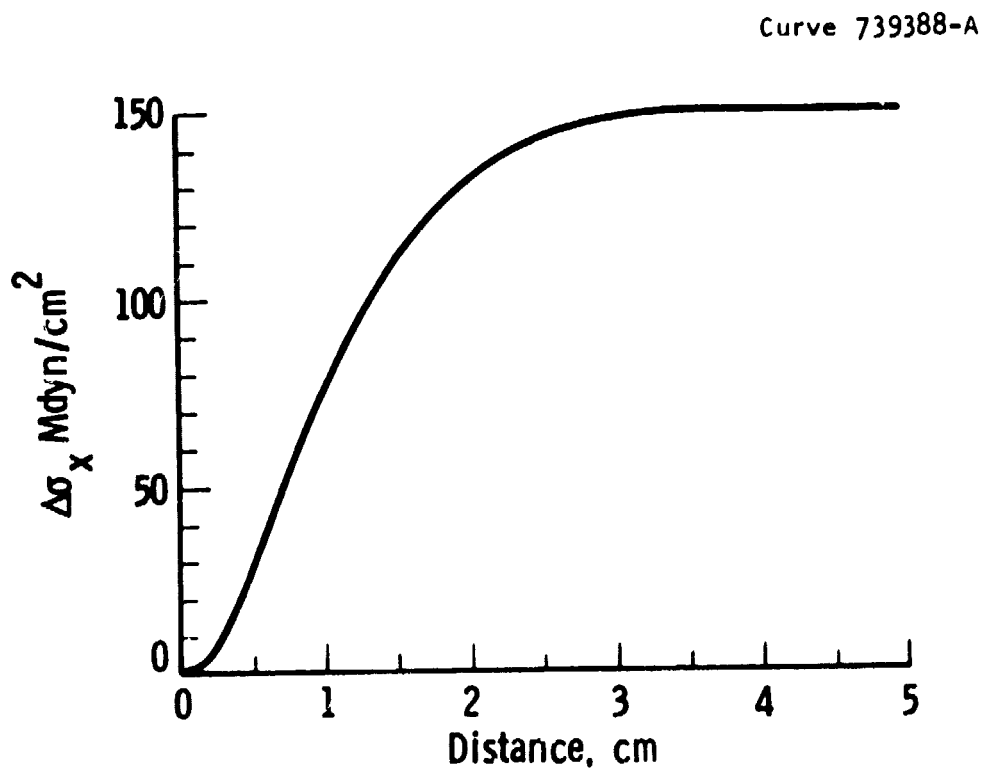


Figure 2. End effect region of constant stress profile.

lid/shield design efforts in that the design itself may be separable into two regions: one near the growth front and one further up the crystal.

The second synthetic temperature profile was intended to show how stresses caused by changes in $(\alpha T)''$ affect adjacent regions of the crystal. The temperature profile used for the analysis was composed of two zero stress segments with the transition at the midpoint of the finite element mesh. Thus $(\alpha T)'' \approx 0$ everywhere, but all the higher derivatives were essentially infinite at the midpoint to give an effective delta function for thermal stress generation.

The results of the WECAN calculations are shown in Figure 3; 3a is the temperature distribution used as input for the WECAN analysis, and 3b is the resulting σ_x and σ_y . The effect of discontinuity in the curvature of the profile obviously spreads over a significant region of the crystal. Again, the σ_x distribution is approximately a Gaussian with a characteristic length of the ribbon half-width.

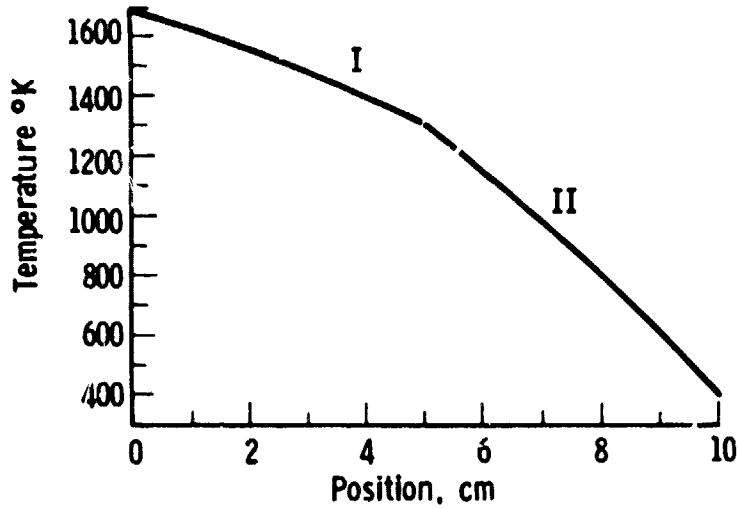
The importance of the results in this run lie in understanding the interaction of different regions of the $(\alpha T)''$ curve. In the previous analysis of web growth configurations, it was obvious that there was a connection between the stress components and the $(\alpha T)''$ values, but it was certainly not as simple as implied by equation 1. The present result indicates that an averaging (or perhaps a convolution) analysis is more appropriate but further gives some indication as to the magnitude of the characteristic distance.

3.1.2 Design of J419 Growth Configuration

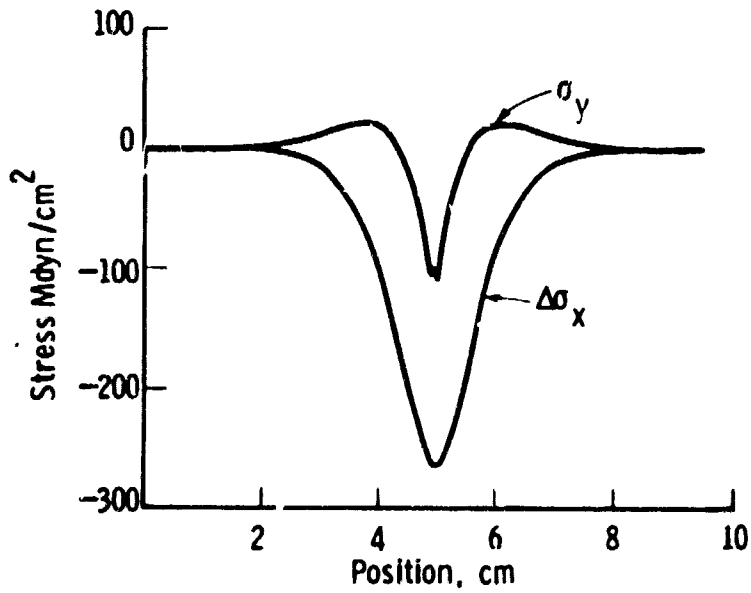
Analysis of the stress distribution and buckling characteristics of dendritic web growth configurations suggested that a major contribution to the buckling comes from a large peak in σ_x which occurred near the point where the web left the shield stack. Furthermore, there were several positive local maxima in the lid region of the crystal. The results of the runs with synthetic temperature

ORIGINAL PAGE IS
OF POOR QUALITY

Curve 739389-A



A. Temperature Profile



B. Resulting Stresses

Figure 3. Stresses generated by abruptly changing zero stress temperature profiles.

profiles suggested that some additional localized heating was needed near the growth front while maintaining the loss to furnace ambient. In addition, losses further along the crystal should be reduced to lower the large x-stress peak. These design requirements seemed to translate into a relatively thick, hot lid with a relatively tall shield stack having shield slots of increasing width.

The resulting configuration is shown in Figure 4. The lid itself is thicker -- .5 inch instead of the .38 inch or .25 inch lid used in a previous configuration. Surmounting the lid are four shields with slot openings arranged so that the web at the growth front has a 25.6° clear view of the cold furnace interior. This configuration was analyzed for thermal stresses using lid and shield temperatures deduced from measurements on other configurations. The stress calculations indicated that the $\Delta\sigma_x$ peak was about half the magnitude of previously calculated values and the σ_y value at the interface was comparable with previous calculations.

On the basis of the calculated thermal stresses, a full buckling analysis was performed on the model. The results indicated that a 150 μm thick web crystal would not buckle at widths narrower than 38 mm. This was a substantial improvement over previous designs and the decision was made to fabricate a set of lids and shields that would give a real growth system representing the design analyzed with the models.

The initial run of the configuration included thermocouples in the lid, bottom shield, and top shield. The measured temperatures were consistent with the temperatures assumed for the stress and buckling. More important, however, was the result that in the initial run an unbuckled crystal was grown to a width of 35 mm, although the thickness was only 125 μm . In subsequent runs, thicker web (190 μm) was grown to a width of 44 mm without buckling and to 49.9 mm with only slight deformation. These width and thickness values are in almost perfect agreement with the buckling predictions.

ORIGINAL PAGE IS
OF POOR QUALITY

Dwg. 7767A15

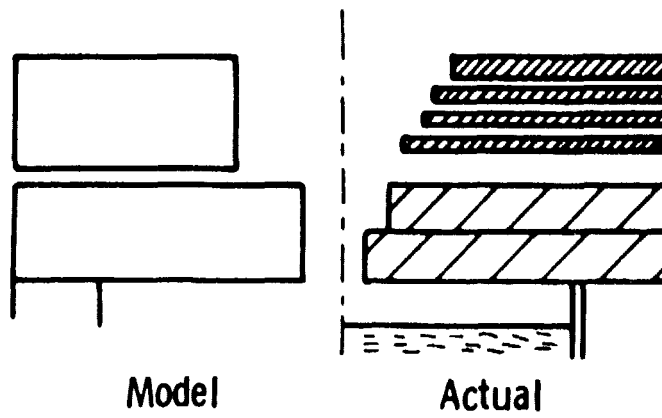


Figure 4. J419 configuration.

3.2 New Experimental Web Growth Facility

The New Experimental Web Growth Facility (N-Furnace) was operated on a regular basis. The major objectives of these experiments were to "tune in" the shield and work coil positions for simultaneous growth with melt replenishment and to evaluate the performance of the melt level sensing and control systems. A J98M3 lid and shield configuration, adapted for melt replenishment by the addition of feed and laser holes, was used for these experiments. This configuration was designed for width limitation and the growth behavior had been well-characterized in the WA and WB furnace facilities, although not under conditions of constant melt level.

During the initial runs, installation of the melt level sensing circuitry had not yet been completed, so that replenishment was carried out with manually set feed rates. The first step was to establish the end shield settings for various replenishment rates so that sufficiently high temperatures were maintained in the feed compartment of the crucible to melt the pellets at the required rate. At the same time, growth behavior was tested at these shield settings in order to establish what feed rates could be achieved without compromising web growth, i.e., the amount of shielding that could be used without seriously perturbing the temperature distribution in the growth region of the melt. These experiments indicated that for web widths of about 2.5 cm, full replenishment rates could be accomplished without difficulty, but that the shielding required for feed rates needed for 3 cm or greater width could begin to affect the temperature distribution in the growth region adversely. This effect can be compensated for by a slight modification of the lid slot geometry, as subsequently proved by experiment.

During this period, installation of the melt level sensing circuitry was completed and tested during growth experiments. It performed as designed but, on the basis of several experimental runs, it was decided that greater sensitivity in the sensing circuit would be

desirable, i.e., the control band was too wide. Another desirable modification is an adjustable upper limit on the feed rate so that it cannot exceed the rate at which pellets melt easily. Minor design changes were made and are being implemented.

As modified, the new furnace facility will enable growth experiments to be carried out under completely controlled long-term, steady-state thermal conditions.

4. CONCLUSIONS

For the first time, the modeling effort was applied to the a priori design of a new low-stress lid and shield configuration. Experimental evaluation gave results consistent with the predictions of the model and confirmed the validity of the models and their usefulness as design tools. At the same time, the modeling effort has greatly enhanced our understanding of the effects on web growth of some rather subtle variations in temperature distribution.

The New Experimental Web Growth Facility, which incorporates all the functions needed for long-term, steady-state growth conditions, will allow experiments to be carried out under known constant reproducible thermal conditions.

5. PLANS AND FUTURE WORK

During development of the J419 configuration, one inadequacy became apparent: the present model used to calculate the temperature distribution in the web considers the entire shield stock as one lumped element. This approach was adequate when only one or two shields were modeled, but is much less satisfactory when a multi shield assembly such as the J419 is modeled. There appears to be relatively direct ways to modify the web temperature model and this will be attempted in the next quarter.

The New Facility will be used to test new growth configurations under controlled, steady-state conditions.

6. NEW TECHNOLOGY

No new technology is reportable for the period covered.

7. REFERENCE

1. Boley, B.A. and Weiner, J. H., Theory of Thermal Stresses, p. 323, Wiley, New York, London, Sidney (1960).

8. ACKNOWLEDGEMENTS

We would like to thank H. C. Foust, E. P. A. Metz, L. G. Stampahar, S. Edlis, W. B. Stickel, and W. Chalmers for their contributions to the web growth studies.

9. PROGRAM SCHEDULE AND COSTS

9.1 Updated Program Plan

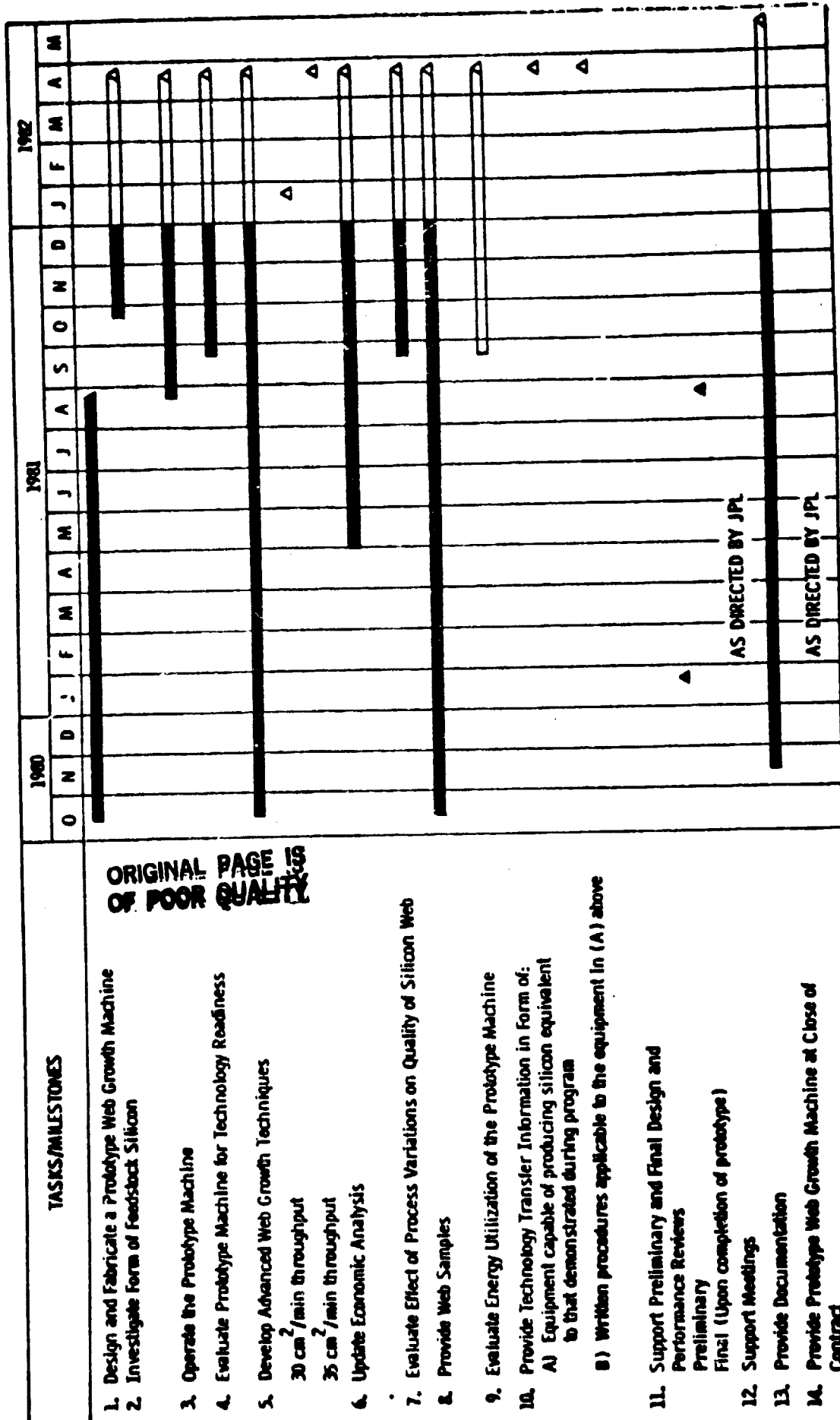
9.1.1 Milestone Chart (see page 17)

9.1.2 Program Cost Summary (see page 16)

9.1.3 Program Labor Summary (see page 19)

9.2 Man-Hours and Costs

Man-hours		Costs	
Previous	18,566	Previous	847,589
This Period	4,314	This Period	186,933
Cumulative	22,880	Cumulative	1,034,522

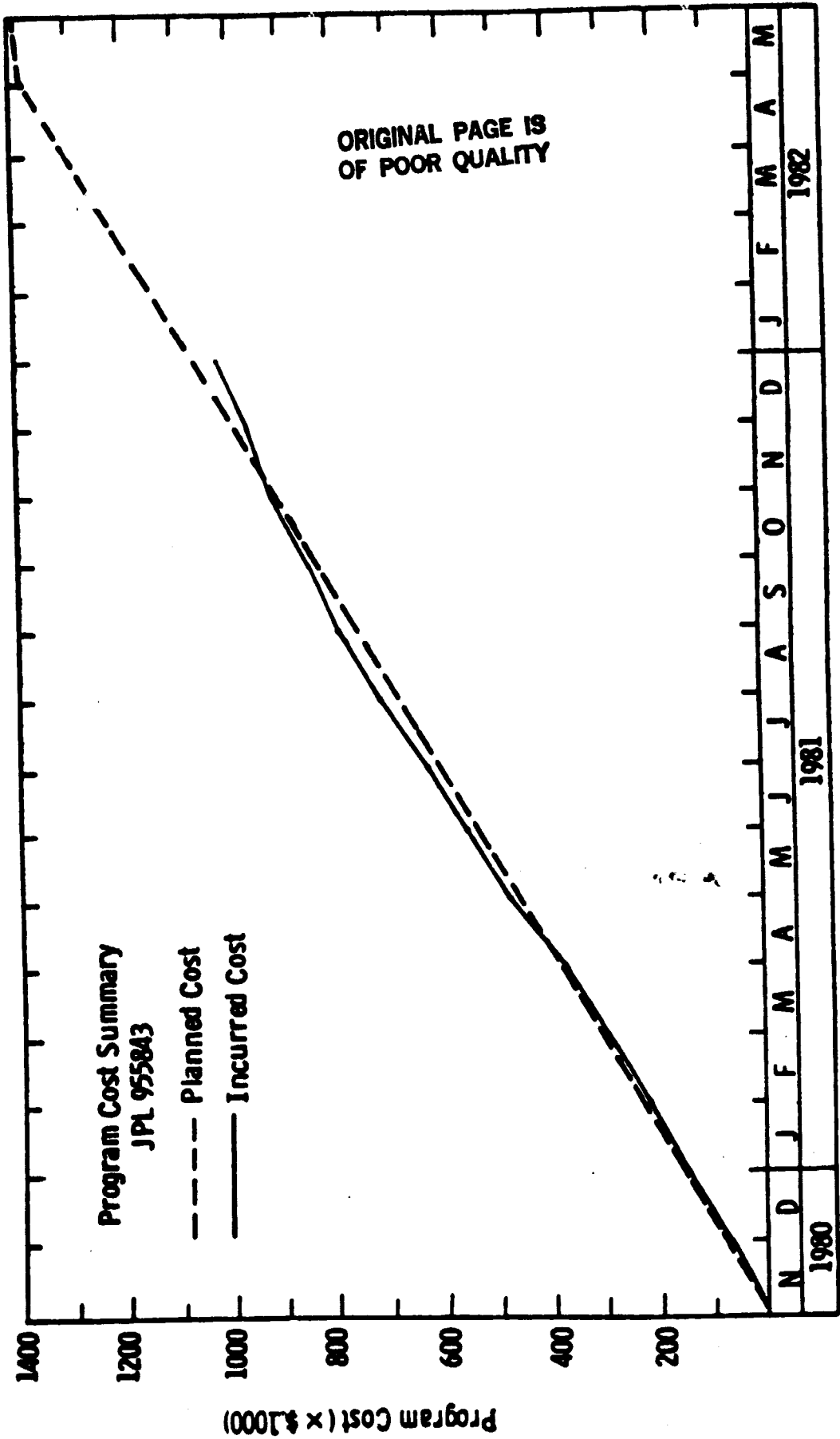


ORIGINAL PAGE OF POOR QUALITY

AS DIRECTED BY JPL

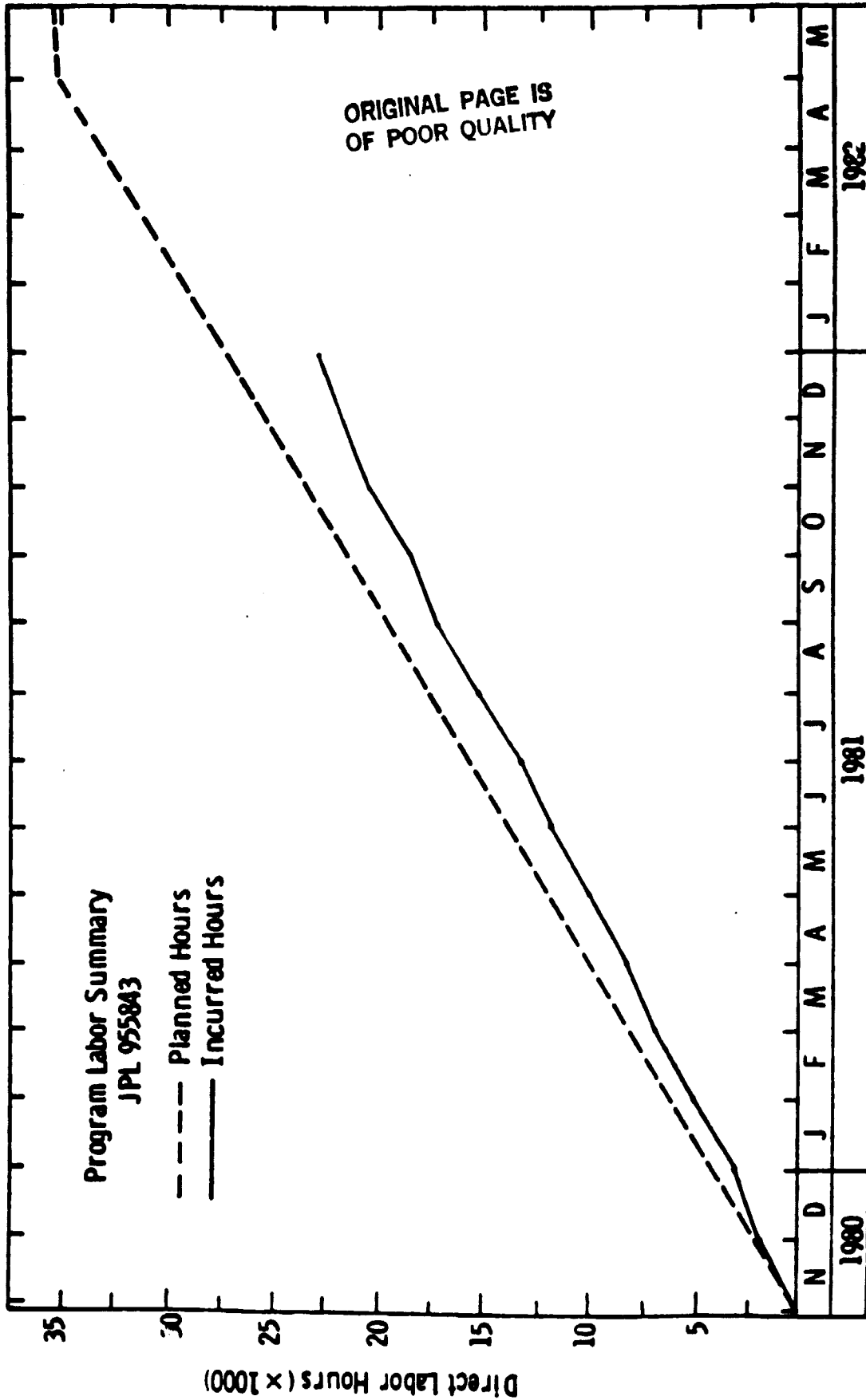
AS DIRECTED BY JPL

Curve 728214-8



Contract Months

Curve 728215-8



Contract Months